

The terrestrial biosphere as a net source of greenhouse gases to the atmosphere

Hanqin Tian¹, Chaoqun Lu^{1,2}, Philippe Ciais³, Anna M. Michalak⁴, Josep G. Canadell⁵, Eri Saikawa⁶, Deborah N. Huntzinger⁷, Kevin R. Gurney⁸, Stephen Sitch⁹, Bowen Zhang¹, Jia Yang¹, Philippe Bousquet³, Lori Bruhwiler¹⁰, Guangsheng Chen¹¹, Edward Dlugokencky¹⁰, Pierre Friedlingstein¹², Jerry Melillo¹³, Shufen Pan¹, Benjamin Poulter¹⁴, Ronald Prinn¹⁵, Marielle Saunois³, Christopher R. Schwalm^{7,16} & Steven C. Wofsy¹⁷

The terrestrial biosphere can release or absorb the greenhouse gases, carbon dioxide (CO₂), methane (CH₄) and nitrous oxide (N₂O), and therefore has an important role in regulating atmospheric composition and climate¹. Anthropogenic activities such as land-use change, agriculture and waste management have altered terrestrial biogenic greenhouse gas fluxes, and the resulting increases in methane and nitrous oxide emissions in particular can contribute to climate change^{2,3}. The terrestrial biogenic fluxes of individual greenhouse gases have been studied extensively^{4–6}, but the net biogenic greenhouse gas balance resulting from anthropogenic activities and its effect on the climate system remains uncertain. Here we use bottom-up (inventory, statistical extrapolation of local flux measurements, and process-based modelling) and top-down (atmospheric inversions) approaches to quantify the global net biogenic greenhouse gas balance between 1981 and 2010 resulting from anthropogenic activities and its effect on the climate system. We find that the cumulative warming capacity of concurrent biogenic methane and nitrous oxide emissions is a factor of about two larger than the cooling effect resulting from the global land carbon dioxide uptake from 2001 to 2010. This results in a net positive cumulative impact of the three greenhouse gases on the planetary energy budget, with a best estimate (in petagrams of CO₂ equivalent per year) of 3.9 ± 3.8 (top down) and 5.4 ± 4.8 (bottom up) based on the GWP100 metric (global warming potential on a 100-year time horizon). Our findings suggest that a reduction in agricultural methane and nitrous oxide emissions, particularly in Southern Asia, may help mitigate climate change.

The concentration of atmospheric CO₂ has increased by nearly 40% since the start of the industrial era, while CH₄ and N₂O concentrations have increased by 150% and 20%, respectively^{3,7,8}. Although thermogenic sources (for example, fossil fuel combustion and usage, cement production, geological and industrial processes) represent the single largest perturbation of climate forcing, biogenic sources and sinks also account for a significant portion of the land–atmosphere exchange of these gases. Land biogenic greenhouse gas (GHG) fluxes are those originating from plants, animals and microbial communities, with changes driven by both natural and anthropogenic perturbations (see Methods). Although the biogenic fluxes of CO₂, CH₄ and N₂O have been individually measured and simulated at various spatial and temporal scales, an overall GHG balance of the terrestrial biosphere is lacking³. But simultaneous quantification of the fluxes of these three gases is needed for developing effective climate change mitigation strategies^{9,10}.

In the analysis that follows, we use a dual-constraint approach from 28 bottom-up (BU) studies and 13 top-down (TD) atmospheric inversion studies to constrain biogenic fluxes of the three gases. We generate decadal mean estimates and s.d. of CO₂, CH₄ and N₂O fluxes (mean \pm s.d., with s.d. being the square root of the quadratic sum of standard deviations reported by individual studies) in land biogenic sectors by using the BU and TD ensembles as documented in Extended Data Table 1 and Supplementary Table 2. Grouping GHG fluxes by sector may not precisely separate the contributions of human activities from natural components. For instance, wetland CH₄ emission is composed of a natural component (background emissions) and an anthropogenic contribution (for example, emissions altered by land use and climate change). Therefore, in this study, the anthropogenic contribution to the biogenic flux of each GHG is distinguished by removing modelled pre-industrial emissions from contemporary GHG estimates. To quantify the human-induced net biogenic balance of these three GHGs and its impact on the climate system, we use CO₂ equivalent units (CO₂ equiv.) based on the global warming potentials on a 100-year time horizon⁷ (GWP100; GWP defines the cumulative impacts that the emission of 1 g CH₄ or N₂O could have on the planetary energy budget relative to 1 g reference CO₂ gas over a certain period of years). This choice has been driven by the policy options being considered when dealing with biogenic GHG emissions and sinks^{7,11}. To address the changing relative importance of each gas as a function of the selected time frame, a supplementary calculation based on GWP metrics for a 20-year time horizon is also provided (GWP20; Table 1 and Methods).

We first examine the overall biogenic fluxes of all three gases in the terrestrial biosphere during the period 2001–10 ('the 2000s'; Fig. 1). The overall land biogenic CH₄ emissions estimated by TD and BU are very similar, 325 ± 39 Tg C yr⁻¹ and 326 ± 43 Tg C yr⁻¹ (1 Tg = 10¹² g), respectively. Among the multiple land biogenic CH₄ sources (Extended Data Table 1), natural wetlands were the largest contributor, accounting for 40%–50% of total CH₄ emissions during the 2000s, while rice cultivation contributed about 10%. The remaining CH₄ emissions were from ruminants (~20%), landfills and waste (~14%), biomass burning (~4%–5%), manure management (~2%), and termites, wild animals and others (~6%–10%). Both TD and BU results suggest a global soil CH₄ sink that offsets approximately 10% of global biogenic CH₄ emissions, but this flux is poorly constrained, especially by atmospheric inversions, given its distributed nature and small magnitude.

¹International Center for Climate and Global Change Research, School of Forestry and Wildlife Sciences, Auburn University, Auburn, Alabama 36849, USA. ²Department of Ecology, Evolution, and Organismal Biology, Iowa State University, Iowa 50011, USA. ³Laboratoire des Sciences du Climat et de l'Environnement, 91191 Gif sur Yvette, France. ⁴Department of Global Ecology, Carnegie Institution for Science, Stanford, California 94305, USA. ⁵Global Carbon Project, CSIRO Oceans and Atmosphere Research, GPO Box 3023, Canberra, Australian Capital Territory 2601, Australia. ⁶Department of Environmental Sciences, Emory University, Atlanta, Georgia 30322, USA. ⁷School of Earth Sciences and Environmental Sustainability, Northern Arizona University, Flagstaff, Arizona 86011, USA. ⁸School of Life Sciences, Arizona State University, Tempe, Arizona 85287, USA. ⁹College of Life and Environmental Sciences, University of Exeter, Exeter EX4 4RJ, UK. ¹⁰NOAA Earth System Research Laboratory, Global Monitoring Division, Boulder, Colorado 80305, USA. ¹¹Environmental Science Division, Oak Ridge National Laboratory, Oak Ridge, Tennessee 37831, USA. ¹²College of Engineering, Mathematics and Physical Sciences, University of Exeter, Exeter EX4 4QF, UK. ¹³The Ecosystems Center, Marine Biological Laboratory, Woods Hole, Massachusetts 02543, USA. ¹⁴Institute of Ecosystems and Department of Ecology, Montana State University, Bozeman, Montana 59717, USA. ¹⁵Center for Global Change Science, Massachusetts Institute of Technology, Cambridge, Massachusetts 02139, USA. ¹⁶Woods Hole Research Center, Falmouth, Massachusetts 02540, USA. ¹⁷Department of Earth and Planetary Science, Harvard University, 29 Oxford Street, Cambridge, Massachusetts 02138, USA.

Table 1 | Human-induced biogenic GHG emissions from the terrestrial biosphere based on GWP100 and GWP20 metrics

Metric	Human-induced GHG (\pm s.d.) (Pg CO ₂ equiv. yr ⁻¹)					
	1980s		1990s		2000s	
	TD	BU	TD	BU	TD	BU
GWP100						
CH ₄ source	7.5 (\pm 1.8)	7.9 (\pm 1.5)	7.4 (\pm 1.8)	6.9 (\pm 1.6)	7.4 (\pm 1.5)	7.5 (\pm 1.7)
N ₂ O source		2.8 (\pm 1.9)	1.6 (\pm 0.6)	2.9 (\pm 0.7)	2.2 (\pm 0.6)	3.3 (\pm 0.7)
CO ₂ sink	-1.4 (\pm 3.9)	-1.2 (\pm 4.0)	-3.2 (\pm 3.8)	-2.1 (\pm 4.1)	-5.8 (\pm 3.4)	-5.3 (\pm 4.5)
Overall GHG balance		9.4 (\pm 4.7)	5.9 (\pm 4.3)	7.7 (\pm 4.4)	3.9 (\pm 3.8)	5.4 (\pm 4.8)
Proportion of land CO ₂ sink being offset		-860%	-290%	-460%	-170%	-200%
GWP20						
CH ₄ source	22.6 (\pm 5.4)	23.6 (\pm 4.6)	22.2 (\pm 5.5)	20.8 (\pm 4.7)	22.3 (\pm 4.6)	22.5 (\pm 5.1)
N ₂ O source		2.8 (\pm 1.9)	1.6 (\pm 0.6)	2.9 (\pm 0.7)	2.2 (\pm 0.6)	3.3 (\pm 0.7)
CO ₂ sink	-1.4 (\pm 3.9)	-1.2 (\pm 4.0)	-3.2 (\pm 3.8)	-2.1 (\pm 4.1)	-5.8 (\pm 3.4)	-5.3 (\pm 4.5)
Overall GHG balance		25.2 (\pm 6.4)	20.7 (\pm 6.7)	21.5 (\pm 6.3)	18.7 (\pm 5.8)	20.4 (\pm 6.8)
Proportion of land CO ₂ sink being offset		-2,120%	-760%	-1,110%	-430%	-480%

Shown are estimated human-induced biogenic fluxes of CO₂, CH₄ and N₂O in the terrestrial biosphere for the 1980s, 1990s and 2000s based on global warming potential on 100-year and 20-year time horizons (GWP100 and GWP20, respectively). Numbers in parenthesis represent 1 s.d. (standard deviation). TD and BU stand for top-down and bottom-up estimates, respectively. The percentage numbers represent the proportion of land CO₂ sink that has been offset by human-induced CH₄ and N₂O emissions in the terrestrial biosphere. Detailed data sources and literature cited are provided in Supplementary Information.

Global biogenic N₂O emissions were estimated to be 12.6 \pm 0.7 Tg N yr⁻¹ and 15.2 \pm 1.0 Tg N yr⁻¹ by TD and BU methods, respectively. Natural ecosystems were a major source, contributing ~55%–60% of all land biogenic N₂O emissions during the 2000s, the rest being from agricultural soils (~25%–30%), biomass burning (~5%), indirect emissions (~5%), manure management (~2%), and human sewage (~2%).

The estimates of the global terrestrial CO₂ sink in the 2000s are -1.6 \pm 0.9 petagrams of carbon a year (where 1 Pg = 10¹⁵ g) (TD) and -1.5 \pm 1.2 Pg C yr⁻¹ (BU). This estimate is comparable with the most recent estimates⁴, but incorporates more data sources (Supplementary Table 1).

Some CH₄ and N₂O emissions were present during pre-industrial times, while the global pre-industrial land CO₂ uptake was approximately in balance with the transport of carbon by rivers to the ocean and a compensatory ocean CO₂ source¹². Thus, the net land-atmosphere CO₂ flux reported here represents fluxes caused by human activities. In contrast, for CH₄ and N₂O only the difference between current and pre-industrial emissions represents net drivers of anthropogenic climate change. When subtracting modelled pre-industrial biogenic CH₄ and N₂O emissions of 125 \pm 14 Tg C yr⁻¹ and 7.4 \pm 1.3 Tg N yr⁻¹, respectively, from the contemporary estimates (see Methods), we find

the heating capacity of human-induced land biogenic CH₄ and N₂O emissions is opposite in sign and equivalent in magnitude to 1.7 (TD) and 2.0 (BU) times that of the current (2000s) global land CO₂ sink using 100-year GWPs (Fig. 1, Table 1). Hence there is a net positive cumulative impact of the three GHGs on the planetary energy budget, with our 'best estimate' being 3.9 \pm 3.8 Pg CO₂ equiv. yr⁻¹ (TD) and 5.4 \pm 4.8 Pg CO₂ equiv. yr⁻¹ (BU).

An alternative GWP metric (for example, GWP20 instead of GWP100) changes the relative importance of each gas, and gives a different view of the potential of various mitigation options¹¹. Using GWP20 values, the radiative forcing of contemporary (2000s) human-induced biogenic CH₄ emission alone is 3.8 (TD) or 4.2 (BU) times that of the land CO₂ sink in magnitude but opposite in sign, much larger than its role using the GWP100 metric (Table 1). Therefore, cutting CH₄ emissions is an effective pathway for rapidly reducing GHG-induced radiative forcing and the rate of climate warming in a short time frame^{8,11}.

On a 100-year time horizon, the cumulative radiative forcing of agricultural and waste emissions alone, including CH₄ from paddy fields, manure management, ruminants, and landfill and waste, along with N₂O emissions from crop cultivation, manure management, human

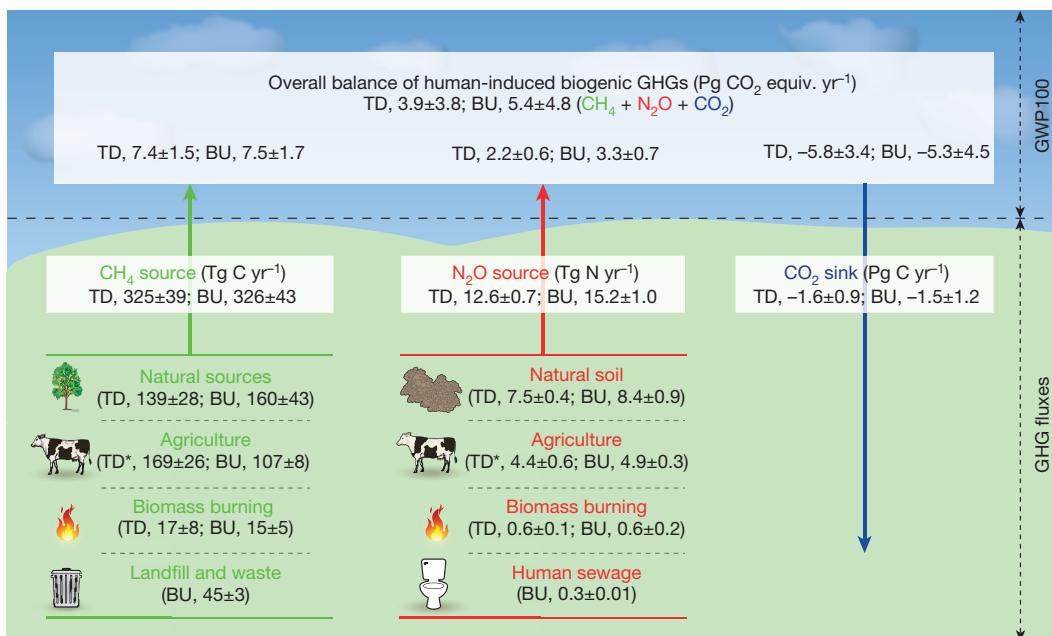


Figure 1 | The overall biogenic GHG balance of the terrestrial biosphere in the 2000s. Top-down (TD) and bottom-up (BU) approaches are used to estimate land CO₂ sink, CH₄ and N₂O fluxes for four major categories merged from 14 sectors (Extended Data Table 1). Global warming potential (GWP100) is calculated after removing pre-industrial biogenic emissions of CH₄ (125 \pm 14 Tg C yr⁻¹) and N₂O (7.4 \pm 1.3 Tg N yr⁻¹). Negative values indicate GHG sinks and positive values indicate GHG sources. TD* indicates estimates of agricultural CH₄ and N₂O emissions that include CH₄ sources from landfill and waste, and an N₂O source from human sewage, respectively.

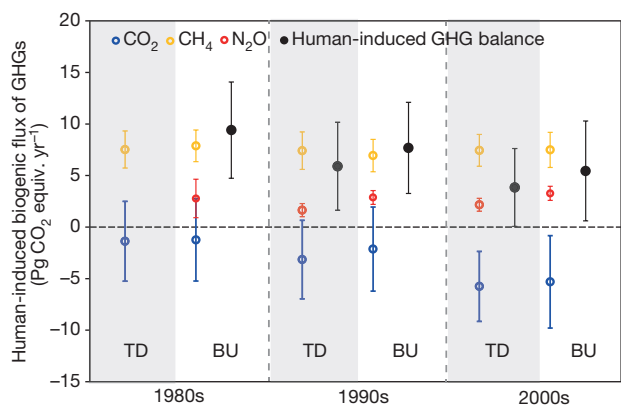


Figure 2 | Changes in the decadal balance of human-induced biogenic GHGs in the past three decades (based on GWP100). Data points show individual gases (blue for CO₂, yellow for CH₄, and red for N₂O) and net human-induced GHG balance (black) derived from biogenic sources with pre-industrial biogenic CO₂ sink, and CH₄ and N₂O emissions removed. Error bars, ±s.d. calculated from various estimate ensembles.

sewage and indirect emissions, are estimated to be 7.9 ± 0.5 Pg CO₂ equiv. yr⁻¹ (BU) and 8.2 ± 1.0 Pg CO₂ equiv. yr⁻¹ (TD) for the 2000s, offsetting the human-induced land CO₂ sink by 1.4 to 1.5 times, respectively. In other words, agriculture and waste are the largest contributor to this twofold offset of the land CO₂ sink.

We further examine the change of human-induced biogenic GHG fluxes over past three decades (Fig. 2, Table 1). The net biogenic GHG source shows a decreasing trend of 2.0 Pg CO₂ equiv. yr⁻¹ per decade ($P < 0.05$), primarily due to an increased CO₂ sink—(2.2 Pg CO₂ equiv. yr⁻¹ per decade (TD) and 2.0 Pg CO₂ equiv. yr⁻¹ per decade (BU), $P < 0.05$)—as driven by a combination of increasing atmospheric CO₂ concentrations, forest regrowth, and nitrogen deposition³. The net emissions of CO₂ from tropical deforestation, included in the above net land CO₂ sink estimates, were found to decline or remain stable owing to reduced deforestation and increased forest regrowth¹³. However, one recent study based on

satellite observations¹⁴ suggests that the decreased deforestation in Brazil has been offset by an increase in deforestation in other tropical countries during 2000–12.

There is no clear decadal trend in total global biogenic CH₄ emissions from 1981 to 2010⁵. Since 2007, increased CH₄ emissions seem to result in a renewed and sustained increase of atmospheric CH₄, although the relative contribution of anthropogenic and natural sources is still uncertain^{15–17}. The BU estimates suggest an increase in human-induced biogenic N₂O emissions since 1980, at a rate of 0.25 Pg CO₂ equiv. yr⁻¹ per decade ($P < 0.05$), mainly due to increasing nitrogen deposition and nitrogen fertilizer use, as well as climate warming¹⁸. With pre-industrial emissions removed, the available TD estimates of N₂O emissions during 1995–2008 reflect a similar positive trend, although they cover a shorter period¹⁹.

The human-induced biogenic GHG fluxes vary by region (Fig. 3). Both TD and BU approaches indicate that human-caused biogenic fluxes of CO₂, CH₄ and N₂O in the biosphere of Southern Asia (Fig. 3) led to a large net climate warming effect, because the 100-year cumulative effects of CH₄ and N₂O emissions together exceed that of the terrestrial CO₂ sink. Southern Asia has about 90% of the global rice fields²⁰ and represents more than 60% of the world's nitrogen fertilizer consumption²¹, with 64%–81% of CH₄ emissions and 36%–52% of N₂O emissions derived from the agriculture and waste sectors (Supplementary Table 3). Given the large footprint of agriculture in Southern Asia, improved fertilizer use efficiency, rice management and animal diets could substantially reduce global agricultural N₂O and CH₄ emissions^{22,23}.

Africa is estimated to be a small terrestrial biogenic CO₂ sink (BU) or a CO₂-neutral region (TD), but it slightly warms the planet when accounting for human-induced biogenic emissions of CH₄ and N₂O, which is consistent with the finding of a recent study²⁴. South America is estimated to be neutral or a small sink of human-induced biogenic GHGs, because most current CH₄ and N₂O emissions in this region were already present during the pre-industrial period, and therefore do not represent new emissions since the pre-industrial era. Using the GWP100 metric, CO₂ uptake in North America and Northern Asia is almost equivalent in magnitude or even larger

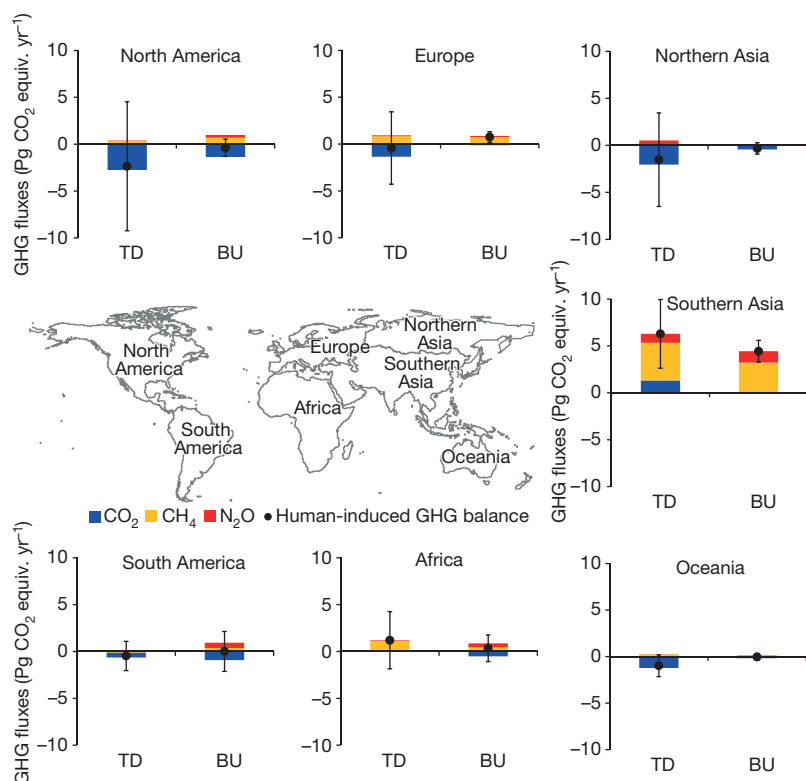


Figure 3 | The balance of human-induced biogenic GHGs for different continents in the 2000s (based on GWP100). Blue bars represent CO₂ flux, yellow CH₄ flux and red for N₂O flux with pre-industrial fluxes removed. Black dots indicate net human-induced GHG balance; error bars, ±s.d. of estimate ensembles.

than human-caused biogenic CH₄ and N₂O emissions but opposite in sign, implying a small but significant role of the land biosphere in mitigating climate warming. Europe's land ecosystem is found to play a neutral role, similar to a previous synthesis study⁹ using both BU and TD approaches.

Compared to global estimations, much more work on regional GHG budgets is needed^{18,19}, particularly for tropical areas, as large uncertainty is revealed in both TD- and BU-derived GHG estimations. TD methods are subject to large uncertainties in their regional attribution of GHG fluxes to different types of sources. Furthermore, some TD estimates used BU values as priors, and may be heavily influenced by these assumed priors in regions where atmospheric observations are sparse. In contrast, BU approaches are able to consider region-specific disturbances and drivers (for example, insects and disease outbreaks) that are important at regional scale but negligible at global scale. However, the shortcoming of BU estimates is that they may not be consistent with the well-observed global atmospheric growth rates of GHGs. Also, accurate BU assessments are hindered by our limited understanding of microbial and below-ground processes and the lack of spatially-explicit, time-series data sets of drivers (for example, wildfire, peatland drainage, wetland extent). The magnitudes of human-induced CH₄ and N₂O emissions reported here are more uncertain than the total emissions of these gases because they contain the uncertainty of both pre-industrial emission and contemporary emission estimates (see Methods for additional discussion).

This study highlights the importance of including all three major GHGs in global and regional climate impact assessments, mitigation option and climate policy development. We should be aware of the likely countervailing impacts of mitigation efforts, such as enhanced N₂O emissions with soil carbon sequestration²⁵, increased CO₂ and N₂O emissions with paddy-drying to reduce CH₄ emissions²⁶, enhanced CH₄ emissions with peatland fire suppression and rewetting to reduce CO₂ and N₂O emissions²⁷, and increased indirect emissions from biofuel production²⁸. The future role of the biosphere as a source or sink of GHGs will depend on future land-use intensification pathways and on the evolution of the land CO₂ sinks²⁹. If the latter continues to increase as observed in the past three decades⁴, the overall biospheric GHG balance could be reversed. However, the evolution of the land CO₂ sink remains uncertain, with some projections showing an increasing sink in the coming decades³, while others showing a weakening sink due to the saturation of the CO₂ fertilization effect and positive carbon-climate feedbacks^{3,30}. Increasing land-use intensification using today's practices to meet food and energy demands will probably increase anthropogenic GHG emissions²³. However, the results of this study suggest that adoption of best practices to reduce GHG emissions from human-impacted land ecosystems could reverse the biosphere's current warming role.

Online Content Methods, along with any additional Extended Data display items and Source Data, are available in the online version of the paper; references unique to these sections appear only in the online paper.

Received 19 January; accepted 9 December 2015.

- Lovelock, J. E. & Margulis, L. Atmospheric homeostasis by and for the biosphere: the gaia hypothesis. *Tellus A* **26**, <http://dx.doi.org/10.3402/tellusa.v26i1-2.9731> (1974).
- Vitousek, P. M., Mooney, H. A., Lubchenco, J. & Melillo, J. M. Human domination of Earth's ecosystems. *Science* **277**, 494–499 (1997).
- Ciais, P. et al. in *Climate Change 2013: The Physical Science Basis* (eds Stocker, T. F. et al.) Ch. 6 (Cambridge Univ. Press, 2013).
- Le Quéré, C. et al. Global carbon budget 2013. *Earth Syst. Sci. Data* **6**, 235–263 (2014).
- Kirschke, S. et al. Three decades of global methane sources and sinks. *Nature Geosci.* **6**, 813–823 (2013).
- Davidson, E. A. & Kanter, D. Inventories and scenarios of nitrous oxide emissions. *Environ. Res. Lett.* **9**, 105012 (2014).
- Myhre, G. et al. in *Climate Change 2013: The Physical Science Basis* (eds Stocker, T. F. et al.) Ch. 8 (Cambridge Univ. Press, 2013).
- Montzka, S., Dlugokencky, E. & Butler, J. Non-CO₂ greenhouse gases and climate change. *Nature* **476**, 43–50 (2011).

- Schulze, E. et al. Importance of methane and nitrous oxide for Europe's terrestrial greenhouse-gas balance. *Nature Geosci.* **2**, 842–850 (2009).
- Tian, H. et al. North American terrestrial CO₂ uptake largely offset by CH₄ and N₂O emissions: toward a full accounting of the greenhouse gas budget. *Clim. Change* **129**, 413–426 (2015).
- Allen, M. *Short-lived Promise? The Science and Policy of Cumulative and Short-lived Climate Pollutants* <http://www.oxfordmartin.ox.ac.uk/publications/view/1960> (Oxford Martin Policy Paper, Oxford Martin School, Univ. Oxford, 2015).
- Jacobson, A. R., Mikaloff Fletcher, S. E., Gruber, N., Sarmiento, J. L. & Gloor, M. A joint atmosphere–ocean inversion for surface fluxes of carbon dioxide: 1. Methods and global-scale fluxes. *Glob. Biogeochem. Cycles* **21**, GB1019 (2007).
- Tubiello, F. N. et al. The contribution of agriculture, forestry and other land use activities to global warming, 1990–2012. *Glob. Change Biol.* **21**, 2655–2660 (2015).
- Hansen, M. C. et al. High-resolution global maps of 21st-century forest cover change. *Science* **342**, 850–853 (2013).
- Dlugokencky, E. et al. Observational constraints on recent increases in the atmospheric CH₄ burden. *Geophys. Res. Lett.* **36**, L18803 (2009).
- Rigby, M. et al. Renewed growth of atmospheric methane. *Geophys. Res. Lett.* **35**, L22805, <http://dx.doi.org/10.1029/2008GL036037> (2008).
- Nisbet, E. G., Dlugokencky, E. J. & Bousquet, P. Methane on the rise — again. *Science* **343**, 493–495 (2014).
- Tian, H. et al. Global methane and nitrous oxide emissions from terrestrial ecosystems due to multiple environmental changes. *Ecosyst. Health Sustain.* **1**, 4 (2015).
- Saikawa, E. et al. Global and regional emissions estimates for N₂O. *Atmos. Chem. Phys.* **14**, 4617–4641 (2014).
- Yan, X., Akiyama, H., Yagi, K. & Akimoto, H. Global estimations of the inventory and mitigation potential of methane emissions from rice cultivation conducted using the 2006 Intergovernmental Panel on Climate Change Guidelines. *Glob. Biogeochem. Cycles* **23**, GB2002 (2009).
- FAO. *Current World Fertilizer Trends and Outlook to 2015* <http://www.fao.org/3/a-av252e.pdf> (Food and Agriculture Organization of the United Nations, Rome, 2011).
- Smith, P. et al. in *Climate Change 2014: Mitigation of Climate Change* (eds Edenhofer, O. et al.) Ch. 11, 816–922 (Cambridge Univ. Press, 2014).
- Tilman, D., Balzer, C., Hill, J. & Befort, B. L. Global food demand and the sustainable intensification of agriculture. *Proc. Natl Acad. Sci. USA* **108**, 20260–20264 (2011).
- Valentini, R. et al. A full greenhouse gases budget of Africa: synthesis, uncertainties, and vulnerabilities. *Biogeosciences* **11**, 381–407 (2014).
- Li, C., Frolking, S. & Butterbach-Bahl, K. Carbon sequestration in arable soils is likely to increase nitrous oxide emissions, offsetting reductions in climate radiative forcing. *Clim. Change* **72**, 321–338 (2005).
- Yu, K., Chen, G. & Patrick, W. H. Reduction of global warming potential contribution from a rice field by irrigation, organic matter, and fertilizer management. *Glob. Biogeochem. Cycles* **18**, GB3018 (2004).
- Murdiyasar, D., Hergoualc'h, K. & Verchot, L. Opportunities for reducing greenhouse gas emissions in tropical peatlands. *Proc. Natl Acad. Sci. USA* **107**, 19655–19660 (2010).
- Melillo, J. M. et al. Indirect emissions from biofuels: how important? *Science* **326**, 1397–1399 (2009).
- Canadell, J. G. & Schulze, E. D. Global potential of biospheric carbon management for climate mitigation. *Nature Commun.* **5**, 5282 (2014).
- Stocker, B. D. et al. Multiple greenhouse-gas feedbacks from the land biosphere under future climate change scenarios. *Nature Clim. Change* **3**, 666–672 (2013).

Supplementary Information is available in the online version of the paper.

Acknowledgements This research was supported partially by NASA grants (NNX08AL73G, NNX14AO73G, NNX10AU06G, NNX11AD47G, NNG04GM39C) and NSF grants (AGS 1243232, AGS-1243220, CNH1210360). J.G.C. was supported by the Australian Climate Change Science Program. E.S. was supported by the NOAA Climate Program Office (award NA13OAR4310059). C.R.S. was supported by NASA grants (NNX12AP74G, NNX10AG01A, NNX11A008A). K.R.G. was supported by NSF CAREER (AGS-0846358). R.G.P. was supported by a NASA Upper Atmosphere Research Program AGAGE grant (NNX11AF17G to MIT). This study contributes to the Non-CO₂ Greenhouse Gases Synthesis of NACP (North American Carbon Program), and the Global Carbon Project (a joint project of IGBP, IHDP, WCRP and Diversitas).

Author Contributions H.T. initiated this research and was responsible for the integrity of the work as a whole. H.T. and C.L. performed analysis, calculations and drafted the manuscript. P.C., A.M.M. and J.G.C. contributed to data synthesis and manuscript development. B.Z., J.Y., G.C. and S.P. contributed to data collection and analysis. E.S., D.N.H., K.R.G., S.S., P.B., L.B., E.D., P.F., J.M., B.P., R.G.P., M.S., C.R.S. and S.C.W. contributed to data provision, data processing, or interpretation. All authors discussed and commented on the manuscript.

Author Information Reprints and permissions information is available at www.nature.com/reprints. The authors declare no competing financial interests. Readers are welcome to comment on the online version of the paper. Correspondence and requests for materials should be addressed to H.T. (tianhan@auburn.edu or tian.hanqin@gmail.com).

METHODS

Definition of biogenic GHG fluxes. In this study, we define land biogenic GHG fluxes as those originating from plants, animals, and microbial communities, with changes driven by both natural and anthropogenic perturbations. For example, this analysis considers the biosphere–atmosphere CO₂ flux resulting from the direct and indirect effects of anthropogenic activities, such as land use and management, climate warming, rising atmospheric CO₂, and nitrogen deposition, but excludes CO₂ emissions due to geological processes (for example, volcanic eruption, weathering), fossil fuel combustion, and cement production. Biogenic CH₄ fluxes include land–atmosphere CH₄ emissions by natural wetlands, rice cultivation, biomass burning, manure management, ruminants, termites, landfills and waste, as well as soil CH₄ uptake. Biogenic N₂O emissions include those released from agricultural ecosystems (that is, fertilized soil emission, manure management, and indirect N₂O emission from manure and synthetic nitrogen fertilizer use), natural ecosystems (that is, soil emissions and emissions from nitrogen re-deposition), human sewage, and biomass burning.

Data sources and calculation. We synthesized estimates of biogenic CO₂, CH₄ and N₂O fluxes in the terrestrial biosphere derived from 28 bottom-up (BU) studies and 13 top-down (TD) atmospheric inversion studies for two spatiotemporal domains (global scale during 1981–2010 and continental scale during the 2000s). First, the data we compiled include the most recent estimates of individual GHG gases from multi-model inter-comparison projects (for example, Atmospheric Tracer Transport Model Inter-comparison Project—TransCom³¹, Trends in net land atmosphere carbon exchanges—TRENDY³², and Multi-scale Synthesis and Terrestrial Model Inter-comparison Project—MsTMIP³³). Second, the estimate ensembles included the published global synthesis results that report decadal land–atmosphere GHG exchange during 1981–2010^{4–6}. Third, for those items that lack detailed information from the above estimations (for example, continental estimate of CH₄ emission from rice fields and soil CH₄ sink, Supplementary Table 1), we use multi-source published estimates and a recent process-based modelling result¹⁸. We limit literature reporting the continental GHG estimate to those studies that have close boundary delineation with our definition, and that have gas flux estimates covering all continents. Only part of the global studies we used has provided continental estimates (details on data sources can be found in Supplementary Table 1 and Supplementary Information Section S3).

In Le Quéré *et al.*⁴, net land CO₂ flux is the sum of carbon emission due to land-use change (E_{LUC}) and the residual terrestrial carbon sink (S_{LAND}). Estimates of budget residual, as one of the top-down approaches, are calculated as the sum of E_{LUC} and S_{LAND} (cited from table 7 of Le Quéré *et al.*⁴). Land CO₂ sink estimated by the TRENDY model inter-comparison project³² does not account for land-use effects on terrestrial carbon dynamics, and we therefore add land-use-induced carbon fluxes as estimated by IPCC AR5³ (table 6.3) to obtain the net land carbon sink estimates. However, the land CO₂ sink estimated by the MsTMIP project³⁴ is derived from model simulations considering climate variability, atmospheric CO₂ concentration, nitrogen deposition, as well as land-use change. We directly use its model ensemble estimates in this study. In addition, BU estimates of land CO₂ sink^{4,34} have been adjusted by removing the CO₂ emissions from drained peatland globally^{13,35}, because global land ecosystem models usually overlook this part of carbon loss.

We include TD and BU estimates of CH₄ and N₂O emission from biomass burning. The TD approach (for example, CarbonTracker-CH₄, Bruhwiler *et al.*³⁶) considers all the emission sources and growth rate in atmospheric concentration. For BU estimation (for example, DLEM simulation, Tian *et al.*³⁷), they use historical fire data that is developed from satellite images and the historical record, to drive a process-based land ecosystem model, so the change in fire occurrence is naturally considered. Other BU estimates, for example, GFED (Van der Werf *et al.*³⁸) and EDGAR³⁹, all include peatland fire emissions. We remove pre-industrial CH₄ and N₂O emission that includes sources from biomass burning to estimate human-caused gas fluxes in the terrestrial biosphere. The role of peatland fire in the estimated CO₂ flux is similar to CH₄ and N₂O estimation: fire emission is included in the TD approach and historical fire is included as one of input drivers (or counted as part of land-use change in most BU models—for example, fire occurrence in deforestation and cropland expansion) in some models. Although peatland fire emission caused by human activities is counted in our analysis, like other sectors, we cannot distinguish how much peat fire is caused by human activity since no specific information is available on pre-industrial peatland fire emission.

In summary, this study provides multi-level estimates on biogenic GHG fluxes, including global biogenic fluxes of CO₂, CH₄, and N₂O during 1981–2010, continental-level estimates on biogenic fluxes of CO₂, CH₄ and N₂O over the 2000s, and sector-based estimates on biogenic CH₄ and N₂O fluxes over the 2000s. Extended Data Table 1 shows our estimates of biogenic CH₄ fluxes for 8 sectors and N₂O fluxes for 6 sectors. These sectors are further merged into four major categories for CH₄ and N₂O fluxes, respectively (Fig. 1).

All the raw data and relevant calculations can be found in Supplementary Table 2. Human-induced biogenic CH₄ and N₂O emissions are calculated by subtracting the pre-industrial emissions as estimated below.

Pre-industrial biogenic GHG estimations. Here we provide a description of how we estimated the pre-industrial GHG emissions. For CO₂ flux, since terrestrial ecosystem models assume the net land–air carbon flux in the pre-industrial era is zero and the modelled C sink is solely human-driven, in order to make TD estimates comparable to BU estimates, the CO₂ sink from TransCom simulations³¹ has been adjusted by removing the natural CO₂ sink (0.45 Pg C yr⁻¹)¹² due to riverine transport from land to ocean. This CO₂ sink of 0.45 Pg C yr⁻¹ was allocated to each continent by using continental-scale estimates of riverine carbon export by Ludwig *et al.*⁴⁰ and assuming 100 Tg C yr⁻¹ of organic carbon is buried and 50% of DIC (dissolved inorganic carbon) export is degassing⁴¹.

Human-induced biogenic CH₄ and N₂O emissions are calculated by subtracting the pre-industrial emissions. We define pre-industrial emissions as the GHG source under pre-industrial environmental conditions and land-use patterns, including CH₄ and N₂O emissions from land ecosystems (for example, natural wetlands, forests, grassland, shrublands). The pre-industrial CH₄ estimate (125.4 ± 14.4 Tg C yr⁻¹) is composed of CH₄ emission from natural wetland and vegetation (99.2 ± 14.3 Tg C yr⁻¹ derived from Houweling *et al.*⁴², Basu *et al.*⁴³ and an unpublished result (H.T.) from DLEM model simulation with potential vegetation map (excluding cropland cultivation and other anthropogenic activities)), termites (15 Tg C yr⁻¹, Dlugokencky *et al.*⁴⁴), and wildfire and wild animals (3.75–7.5 Tg C yr⁻¹ each, Dlugokencky *et al.*⁴⁴). Pre-industrial N₂O emission (7.4 ± 1.3 Tg N yr⁻¹) is derived from the estimate of terrestrial N₂O emission (6.6 ± 1.4 Tg N yr⁻¹) by Davidson and Kanter⁶, and a DLEM simulation (H.T., unpublished results) (8.1 ± 1.2 Tg N yr⁻¹) driven by environmental factors at pre-industrial level and a potential vegetation map.

Calculation and interpretation of GWP. GWP is used to define the cumulative impacts that the emission of 1 g CH₄ or N₂O could have on the planetary energy budget relative to 1 g reference CO₂ gas over a certain period (for example, GWP100 and GWP20 for 100 or 20 years). To calculate CO₂ equivalents of the human-induced biogenic GHG balance, we adopt 100-year GWPs of 28 and 265 for CH₄ and N₂O, respectively, and 20-year GWPs of 84 and 264, respectively⁷. These values of GWP20 and GWP100 used in this study do not include carbon–climate feedbacks. The different contributions of each gas to the net GHG balance will vary using different GWP time horizons (for example, GWP20 versus GWP100, see Table 1). In this study, we applied the following equation to calculate the human-induced biogenic GHG balance:

$$\text{GHG} = F_{\text{CO}_2\text{-C}} \frac{44}{12} + F_{\text{CH}_4\text{-C}} \frac{16}{12} \times \text{GWP}_{\text{CH}_4} + F_{\text{N}_2\text{O-N}} \frac{44}{28} \times \text{GWP}_{\text{N}_2\text{O}}$$

Where $F_{\text{CO}_2\text{-C}}$, $F_{\text{CH}_4\text{-C}}$ and $F_{\text{N}_2\text{O-N}}$ are annual exchanges (unit: Pg C yr⁻¹ or Pg N yr⁻¹) of human-induced biogenic CO₂, CH₄ and N₂O between terrestrial ecosystems and the atmosphere based on the mass of C and N, respectively. The fractions 44/12, 16/12 and 44/28 were used to convert the mass of CO₂-C, CH₄-C and N₂O-N into CO₂, CH₄ and N₂O. GWP_{CH_4} (Pg CO₂ equiv. per Pg CH₄) and $\text{GWP}_{\text{N}_2\text{O}}$ (Pg CO₂ equiv. per Pg N₂O) are constants indicating integrated radiative forcing of CH₄ and N₂O in terms of a CO₂ equivalent unit.

Nevertheless, it is noted that adoption of GWP100 to calculate CO₂ equivalent is not fundamentally scientific but depends on a policy perspective. The relative importance of each gas at a certain time period and likely mitigation option could change due to GWP metrics at different time horizon (for example, GWP20 and GWP100 according to Myhre *et al.*⁷, Table 1). For example, CH₄ has a shorter lifetime (~9 years), and its cumulative radiative forcing is equivalent to 84 times the same amount of CO₂ over 20 years, and 28 times the same amount of CO₂ over 100 years. At a 20-year time horizon, anthropogenic CH₄ and N₂O emissions in the 2000s are equivalent to 4.2–4.8 (TD–BU) times the land CO₂ sink in magnitude but opposite in sign, and the net balance of human-induced GHG in the terrestrial biosphere is 20.4 ± 6.8 Pg CO₂ equiv. yr⁻¹ and 18.7 ± 5.8 Pg CO₂ equiv. yr⁻¹ as estimated by BU and TD approaches, respectively. Among them, anthropogenic CH₄ emissions are 7–10 times (BU–TD) as much as N₂O emissions in terms of GWP20. At a 20-year time horizon, the cumulative radiative forcing of contemporary anthropogenic CH₄ emission alone is 3.8–4.2 (TD–BU) times as much as that of the land CO₂ sink but opposite in sign, larger than its role at a 100-year time horizon (1.3–1.4 times the radiative forcing of the CO₂ sink). Therefore, to cut CH₄ emission could rapidly reduce GHG-induced radiative forcing in a short time frame^{7,8,44}.

Statistics. We use mean ± 1 standard deviation (s.d.) to indicate the best estimates and their ranges. Estimate ensembles are grouped for the TD and BU approaches, and the mean value of multiple ensembles is calculated for each gas in a certain region and period. In the TD and BU groups, we assume the individual estimates are independent of each other, and therefore, the s.d. for each ensemble

mean is calculated as the square root of the quadratic sum of s.d.s reported in each estimate.

Sample size. No statistical methods were used to predetermine sample size.

Continental-level estimations and divergence of biogenic-GHG fluxes. Using the TD and BU ensembles, we estimated the net human-induced biogenic GHG balance during the 2000s for 7 continents or regions, which include North America, South America, Europe, Northern Asia, Southern Asia, Africa and Oceania (Fig. 3). Primarily owing to large CH₄ and N₂O emissions, both approaches show that Southern Asia is a net human-induced biogenic GHG source of 6.3 ± 3.7 Pg CO₂ equiv. yr⁻¹ and 4.4 ± 1.2 Pg CO₂ equiv. yr⁻¹ as estimated by TD and BU, respectively, with the GWP100 metric (Supplementary Table 3). Southern Asia has about 90% of the global rice fields and represents over 60% of the world's nitrogen fertilizer consumption. China and India together consume half of the global nitrogen fertilizer²¹. This leads to the highest regional CH₄ and N₂O emissions, as the two approaches consistently reveal. This finding is also consistent with previous studies conducted in China and India^{45–47}. South America was estimated to be a CO₂ sink with a large uncertainty (Supplementary Table 3). Although South America is a large CH₄ and N₂O source, most of these emissions are present at pre-industrial times. Natural wetlands in South America accounted for 31%–40% of global wetland CH₄ emissions in the 2000s, and 26%–30% of the global natural soil N₂O emissions were derived from this region. Therefore, the contribution of this continent to human-induced GHG balance is negligible or acts as a small sink. Likewise, Africa is estimated to be a small CO₂ sink or a CO₂-neutral region, but adding CH₄ and N₂O emissions makes this continent contribute a small positive radiative forcing, slightly warming the planet.

North America and Northern Asia are found to be a neutral region to a net human-induced biogenic GHG sink, with 100-year cumulative radiative forcing of biogenic CH₄ and N₂O emissions fully or partially offsetting that of the land CO₂ sink in this continent (Supplementary Table 3). The largest CO₂ sink was found in North America, ranging from -0.37 ± 0.22 Pg C yr⁻¹ to -0.75 ± 1.87 Pg C yr⁻¹ as estimated by BU and TD, respectively, probably due to a larger area of highly productive and intensively managed ecosystems (for example, forests, woodlands, and pasture) that were capable of sequestering more CO₂. Our estimate falls within the newly-reported CO₂ sink of -0.28 to -0.89 Pg C yr⁻¹ in North America obtained by synthesizing inventory, atmospheric inversions, and terrestrial modelling estimates⁴⁸. Considering the three gases together, TD estimates showed that North America acts as a net GHG sink with a large s.d. (human-induced biogenic GHG of -2.35 ± 6.87 Pg CO₂ equiv. yr⁻¹, Fig. 3 and Supplementary Table 3). By contrast, BU estimates suggested that North America was a small GHG sink of -0.38 ± 0.93 Pg CO₂ equiv. yr⁻¹ based on GWP100. Our estimate is comparable to previous GHG budget syntheses for North America^{10,37}. TD estimates indicated that Oceania and Europe act to give a small negative net radiative forcing over 100 years (-0.98 ± 1.17 and -0.42 ± 3.86 Pg CO₂ equiv. yr⁻¹, respectively), while BU estimates indicated a negligible contribution in Oceania, and a positive net radiative forcing (0.76 ± 0.57 Pg CO₂ equiv. yr⁻¹) in Europe. According to BU estimates, CO₂ emission from drained peatland in Europe accounted for about one-third of the global total during the 2000s³⁵, which partially explains the warming effect of biogenic GHG in this region as revealed by BU.

It is important to note that only human-caused biogenic GHG fluxes are included in this study, and the regional GHG balance will clearly move towards a net source if the emissions related to fossil fuel combustion and usage are taken into account.

Our analyses indicate that the TD and BU estimates show a larger divergence at the continental scale than at the global scale. We note that the high radiative forcing estimate of human-induced biogenic GHG balance (6.30 ± 3.66 Pg CO₂ equiv. yr⁻¹) in the TD approach in Southern Asia is partially because the land biosphere in this region is estimated to be a net CO₂ source of 0.36 Pg C yr⁻¹ with a large s.d. of 0.99 Pg C yr⁻¹ by TransCom inversions^{31,49}. It includes CO₂ sources and sinks from respiration, primary production, disturbances, rivers outgassing, and land-use change. In contrast, most BU estimations using land ecosystem models do not consider the full set of factors responsible for CO₂ release^{32,33}. The discrepancy between TD and BU estimates for Southern Asia may occur for several reasons. First, the land-use history data commonly used for driving terrestrial biosphere models, for example, HYDE⁵⁰ and GLM⁵¹, were reported to overestimate cropland area and cropland expansion rate in China and to under-estimate it in India compared to the regional data set^{52,53}, thus biasing BU estimates of land conversion-induced carbon fluxes. But none of the BU models included in this study conducted global simulation with such a regional data set updated. Second, large uncertainties exist in estimating carbon release due to tropical deforestation^{4,54–57}. Third, carbon emissions due to peat fires and peatland drainage were a large but usually ignored carbon source in tropical Asia (EDGAR 4.2³⁹ and Joosten *et al.*³⁵). In the BU estimates we included, some models consider peat fire by using an input driver of fire regime from satellite images, while most of them do not consider drained

peatland and accelerated SOC (soil organic carbon) decomposition. Therefore, BU models may underestimate the CO₂ emissions from intensively-disturbed areas, resulting in a small CO₂ source of 0.03 ± 0.29 Pg C yr⁻¹. BU estimations show that the net human-induced biogenic GHG balance in Southern Asia turned out to warm the planet with a 100-year cumulative radiative forcing of 4.44 ± 1.17 Pg CO₂ equiv. yr⁻¹.

Net GHG balance in Africa was positive but with a discrepancy between the TD and BU approaches. TD estimates suggested that Africa was a weak source of CO₂ and a strong source of CH₄ and N₂O, resulting in a positive net radiative forcing of 1.20 ± 3.05 Pg CO₂ equiv. yr⁻¹. However, BU ensembles estimated that African terrestrial biosphere acted as a relatively smaller climate warmer (0.34 ± 1.42 Pg CO₂ equiv. yr⁻¹) due to an anthropogenic land sink of CO₂ (-0.52 ± 1.38 Pg CO₂ equiv. yr⁻¹) and a strong source of CH₄ and N₂O. These divergent estimates in Africa occur for several reasons. First, it was difficult to constrain emissions using TD in this region, due to the lack of atmospheric data. No tropical continent is covered by enough atmospheric GHG measurement stations, making the TD results uncertain in those regions, with almost no uncertainty reduction from the prior knowledge assumed before inversion. Second, there were also large uncertainties in BU estimates. Some of the BU models ignored fire disturbance that is likely to result in a carbon source of 1.03 ± 0.22 Pg C yr⁻¹ in Africa^{24,38} and this emission has been partially offset by carbon uptake due to regrowth. Another reason might be the overestimated CO₂ fertilization effect, which could be limited by nutrient availability. Only a few BU models addressed interactive nutrient cycles in their simulation experiments³².

Uncertainty sources and future research needs. A wide variety of methods, such as statistical extrapolations, and process-based and inverse modelling, were applied to estimate CO₂, CH₄ and N₂O fluxes. TD methods are subject to large uncertainties in their regional attribution of GHG fluxes to different type of sources⁵⁸. BU approaches are however limited by our understanding of underlying mechanisms and the availability and quality of input data. In addition, the TD approach is dependent on BU estimates as prior knowledge, especially in the tropics where both uncertainties are very large.

For example, terrestrial CO₂ uptake estimates from process-based model ensembles in Africa, South America, and Southern Asia are larger than those from TD approaches, while smaller than TD estimates in North America, Europe, Oceania and Northern Asia (Fig. 3, Supplementary Table 3). The larger BU CO₂ sink estimate might be related to biased land-use history data, excluded fire emission and CO₂ release due to extreme disturbances such as insect outbreaks and windthrow^{24,32}. Another reason is the lack of fully-coupled carbon–nitrogen cycles in most BU models that overestimate the CO₂ fertilization effect particularly in regions of large biomass and large productivity^{59–61}. However, a larger CO₂ sink observed from tropical regrowth forests compared to intact forests⁵⁵ might be underestimated because few models are capable of capturing CO₂ uptake related to tropical secondary forest management and age structure. The post-disturbance and plantation-induced shift towards rapid carbon accumulation in young forests that were poorly or not represented in terrestrial ecosystem models might be one of the factors responsible for CO₂ sink underestimation as revealed by several studies conducted in mid- and high-latitudes^{62–64}. The modelled ecosystem responses to frequent occurrence of extreme climate events in BU studies are another uncertainty in estimating variations of the land CO₂ sink^{65,66}.

The estimates of terrestrial CH₄ fluxes remain largely uncertain. One major uncertainty in BU wetland CH₄ emission estimate is wetland areal extent data⁶⁷. Global inundated area extent was reported to decline by approximately 6% during 1993–2007 with the largest decrease in tropical and subtropical South America and South Asia⁶⁸. However, the majority of BU models failed either in capturing dynamic inundation area or in simulating inundation and saturated conditions. Tropical emissions, the dominant contributor for global wetland emission, are particularly difficult to quantify owing to sparse observations for both TD (atmospheric mixing ratios) and BU (flux measurements) approaches and large inter-annual, seasonal variability, and a long-term change in the inundation extent for the BU modelling approach^{5,36,68}. At high latitudes, current dynamic inundation data could not well represent permanent wetlands⁶⁷, most of which are occupied by peatland. Because of large soil carbon storage in peatlands, such areas are an important CH₄ source. In addition, a large divergence exists in the estimation of rice field CH₄ emissions (Supplementary Table 2). The estimated global CH₄ emissions from rice fields are sensitive to rice field area, management practices (for example, water regime, fertilizer application), and local climate and soil conditions that directly affect activities of methanotroph and methanogen^{20,69,70}. Models need better representation of CH₄ production and consumption processes modified by agricultural management, such as continuous flooding, irrigation with intermediate drainage, or rainfed⁷⁰.

Compared to CO₂ and CH₄, there have been fewer studies of global N₂O emissions. The TD approach is constrained by sparse or inconsistent measurements

- of atmospheric N₂O mixing ratios^{19,71}. Decadal trends during 1981–2010 from BU approaches were primarily from two process-based models^{18,72}, instead of IPCC methodology based on the N₂O emission factors. The major uncertainty source, therefore, includes data characterizing spatiotemporal variation of reactive nitrogen enrichment, modelling schemes representing multiple nitrogen forms, transformation, and their interactions with other biogeochemical and hydrological cycles, as well as key parameters determining the sensitivity of N₂O emission to temperature, soil moisture, and availability of oxygen^{45,46,72–74}. A large divergence exists in the estimation of natural soil N₂O emission by inventory, empirical and process-based models, implying that our understanding of the processes and their controls remain uncertain^{18,72,75–77}. Tropical areas are the major contributors to large divergence. N₂O sources from tropical undisturbed wetland and drained wetland/peatland are likely to be underestimated⁷⁸.
31. Gurney, K. R., Baker, D., Rayner, P. & Denning, S. Interannual variations in continental-scale net carbon exchange and sensitivity to observing networks estimated from atmospheric CO₂ inversions for the period 1980 to 2005. *Glob. Biogeochem. Cycles* **22**, GB3025 (2008).
 32. Sitch, S. *et al.* Recent trends and drivers of regional sources and sinks of carbon dioxide. *Biogeosciences* **12**, 653–679 (2015).
 33. Huntingger, D. *et al.* The North American carbon program multi-scale synthesis and terrestrial model intercomparison project—part 1: Overview and experimental design. *Geosci. Model Dev.* **6**, 2121–2133 (2013).
 34. Schwalm, C. R. *et al.* Toward “optimal” integration of terrestrial biosphere models. *Geophys. Res. Lett.* **42**, 4418–4428 (2015).
 35. Joosten, H. *The Global Peatland CO₂ Picture: Peatland Status and Drainage Related Emissions in All Countries of the World* http://www.wetlands.org/Portals/0/publications/Report/The%20Global%20Peatland%20CO2%20Picture_web%20Aug%202010.pdf (Greifswald University Wetlands International, Ede, 2010).
 36. Bruhwiler, L. *et al.* CarbonTracker-CH₄: an assimilation system for estimating emissions of atmospheric methane. *Atmos. Chem. Phys.* **14**, 8269–8293 (2014).
 37. Tian, H. *et al.* Contemporary and projected biogenic fluxes of methane and nitrous oxide in North American terrestrial ecosystems. *Front. Ecol. Environ.* **10**, 528–536 (2012).
 38. van der Werf, G. R. *et al.* Global fire emissions and the contribution of deforestation, savanna, forest, agricultural, and peat fires (1997–2009). *Atmos. Chem. Phys.* **10**, 11707–11735 (2010).
 39. EDGAR Emission Database for Global Atmospheric Research (EDGAR) release version 4.2 <http://edgar.jrc.ec.europa.eu/overview.php?v=42> (2014); accessed 2 February 2016.
 40. Ludwig, W., Amiotte-Suchet, P. & Probst, J. ISLSCP II atmospheric carbon dioxide consumption by continental erosion. <http://dx.doi.org/10.3334/ORNLDAAC/1019> (ORNL DAAC, 2011).
 41. Sarmiento, J. & Sundquist, E. Revised budget for the oceanic uptake of anthropogenic carbon dioxide. *Nature* **356**, 589–593 (1992).
 42. Houweling, S., Van der Werf, G., Klein Goldewijk, K., Röckmann, T. & Aben, I. Early anthropogenic CH₄ emissions and the variation of CH₄ and ¹³CH₄ over the last millennium. *Glob. Biogeochem. Cycles* **22**, GB1002 (2008).
 43. Basu, A. *et al.* Analysis of the global atmospheric methane budget using ECHAM-MOZ simulations for present-day, pre-industrial time and the Last Glacial Maximum. *Atmos. Chem. Phys. Discuss.* **14**, 3193–3230 (2014).
 44. Dlugokencky, E. J., Nisbet, E. G., Fisher, R. & Lowry, D. Global atmospheric methane: budget, changes and dangers. *Phil. Trans. R. Soc. A* **369**, 2058–2072 (2011).
 45. Lu, C. & Tian, H. Net greenhouse gas balance in response to nitrogen enrichment: perspectives from a coupled biogeochemical model. *Glob. Change Biol.* **19**, 571–588 (2013).
 46. Tian, H. *et al.* Net exchanges of CO₂, CH₄, and N₂O between China's terrestrial ecosystems and the atmosphere and their contributions to global climate warming. *J. Geophys. Res.* **116**, G02011 (2011).
 47. Banger, K. *et al.* Biosphere–atmosphere exchange of methane in India as influenced by multiple environmental changes during 1901–2010. *Atmos. Environ.* **119**, 192–200 (2015).
 48. King, A. *et al.* North America's net terrestrial CO₂ exchange with the atmosphere 1990–2009. *Biogeosciences* **12**, 399–414 (2015).
 49. Baker, D. *et al.* TransCom 3 inversion intercomparison: impact of transport model errors on the interannual variability of regional CO₂ fluxes, 1988–2003. *Glob. Biogeochem. Cycles* **20**, GB1002, <http://dx.doi.org/10.1029/2004GB002439> (2006).
 50. Goldewijk, K. K. Estimating global land use change over the past 300 years: the HYDE database. *Glob. Biogeochem. Cycles* **15**, 417–433 (2001).
 51. Hurtt, G. *et al.* The underpinnings of land-use history: three centuries of global gridded land-use transitions, wood-harvest activity, and resulting secondary lands. *Glob. Change Biol.* **12**, 1208–1229 (2006).
 52. Liu, M. & Tian, H. China's land cover and land use change from 1700 to 2005: estimations from high-resolution satellite data and historical archives. *Glob. Biogeochem. Cycles* **24**, GB3003 (2010).
 53. Tian, H., Banger, K., Bo, T. & Dadhwal, V. K. History of land use in India during 1880–2010: large-scale land transformations reconstructed from satellite data and historical archives. *Global Planet. Change* **121**, 78–88 (2014).
 54. Friedlingstein, P. *et al.* Update on CO₂ emissions. *Nature Geosci.* **3**, 811–812 (2010).
 55. Pan, Y. *et al.* A large and persistent carbon sink in the world's forests. *Science* **333**, 988–993 (2011).
 56. Harris, N. L. *et al.* Baseline map of carbon emissions from deforestation in tropical regions. *Science* **336**, 1573–1576 (2012).
 57. Archer-Nicholls, S. *et al.* Characterising Brazilian biomass burning emissions using WRF-Chem with MOSAIC sectional aerosol. *Geosci. Model Dev.* **8**, 549–577 (2015).
 58. Peylin, P. *et al.* Global atmospheric carbon budget: results from an ensemble of atmospheric CO₂ inversions. *Biogeosciences* **10**, 6699–6720 (2013).
 59. Thornton, P. E. *et al.* Carbon-nitrogen interactions regulate climate-carbon cycle feedbacks: results from an atmosphere-ocean general circulation model. *Biogeosciences* **6**, 2099–2120 (2009).
 60. Sokolov, A. P. *et al.* Consequences of considering carbon-nitrogen interactions on the feedbacks between climate and the terrestrial carbon cycle. *J. Clim.* **21**, 3776–3796 (2008).
 61. Zaehle, S., Friedlingstein, P. & Friend, A. D. Terrestrial nitrogen feedbacks may accelerate future climate change. *Geophys. Res. Lett.* **37**, L01401 (2010).
 62. Goward, S. N. *et al.* Forest disturbance and North American carbon flux. *Eos Trans. AGU* **89**, 105–106 (2008).
 63. Williams, C. A., Collatz, G. J., Masek, J. & Goward, S. N. Carbon consequences of forest disturbance and recovery across the conterminous United States. *Glob. Biogeochem. Cycles* **26**, GB1005 (2012).
 64. Bellassen, V. *et al.* Reconstruction and attribution of the carbon sink of European forests between 1950 and 2000. *Glob. Change Biol.* **17**, 3274–3292 (2011).
 65. Reichstein, M. *et al.* Climate extremes and the carbon cycle. *Nature* **500**, 287–295 (2013).
 66. Zscheischler, J. *et al.* Impact of large-scale climate extremes on biospheric carbon fluxes: an intercomparison based on MSTMIP data. *Glob. Biogeochem. Cycles* **28**, 585–600 (2014).
 67. Melton, J. *et al.* Present state of global wetland extent and wetland methane modelling: conclusions from a model intercomparison project (WETCHIMP). *Biogeosciences* **10**, 753–788 (2013).
 68. Prigent, C. *et al.* Changes in land surface water dynamics since the 1990s and relation to population pressure. *Geophys. Res. Lett.* **39**, L08403 (2012).
 69. Ren, W. *et al.* Spatial and temporal patterns of CO₂ and CH₄ fluxes in China's croplands in response to multifactor environmental changes. *Tellus B* **63**, 222–240 (2011).
 70. Banger, K., Tian, H. & Lu, C. Do nitrogen fertilizers stimulate or inhibit methane emissions from rice fields? *Glob. Change Biol.* **18**, 3259–3267 (2012).
 71. Reay, D. S. *et al.* Global agriculture and nitrous oxide emissions. *Nature Clim. Change* **2**, 410–416 (2012).
 72. Saikawa, E., Schlosser, C. & Prinn, R. Global modeling of soil nitrous oxide emissions from natural processes. *Glob. Biogeochem. Cycles* **27**, 972–989 (2013).
 73. Bouwman, A. *et al.* Global trends and uncertainties in terrestrial denitrification and N₂O emissions. *Phil. Trans. R. Soc. Lond. B* **368**, 20130112, <http://dx.doi.org/10.1098/rstb.2013.0112> (2013).
 74. Butterbach-Bahl, K., Diaz-Pines, E. & Dannenmann, M. in *Handbook of Global Environmental Pollution* Vol. 1, *Global Environmental Change* 325–334 (Springer, 2014).
 75. Potter, C. S., Matson, P. A., Vitousek, P. M. & Davidson, E. A. Process modeling of controls on nitrogen trace gas emissions from soils worldwide. *J. Geophys. Res. Atmos.* **101**, 1361–1377 (1996).
 76. Xu, X., Tian, H. & Hui, D. Convergence in the relationship of CO₂ and N₂O exchanges between soil and atmosphere within terrestrial ecosystems. *Glob. Change Biol.* **14**, 1651–1660 (2008).
 77. Zhuang, Q. *et al.* Response of global soil consumption of atmospheric methane to changes in atmospheric climate and nitrogen deposition. *Glob. Biogeochem. Cycles* **27**, 650–663 (2013).
 78. Lienggaard, L. *et al.* Extreme emission of N₂O from tropical wetland soil (Pantanal, South America). *Front. Microbiol.* **3**, 1–13 (2012).

Extended Data Table 1 | Decadal estimates of global terrestrial biogenic CO₂, CH₄ and N₂O fluxes

GHG	Sector	1980s		1990s		2000s		
		Top-down	Bottom-up	Top-down	Bottom-up	Top-down	Bottom-up	
CO ₂ (Pg C/yr)	Net land CO₂ sink	-0.4±1.1	-0.3±1.1	-0.9±1.0	-0.6±1.1	-1.6±0.9	-1.5±1.2	
	1) Natural wetland	125.3±43.5	168.8±31.1	112.5±6.0	154.5±36.0	131.3±24.8	162.8±40.1	
	2) Soil sinks	-15.8±6.4	-19.7±14.3	-20.3±0.0	-21.5±14.3	-24.0±6.0	-22.6±14.3	
	3) Termite, Wild animal & Others	27.0±0.4	19.5±3.8	24.0±5.3	19.5±3.8	32.3±10.5	19.5±3.8	
	Natural*	136.5±44.0	168.6±34.5	116.3±8.0	152.5±38.9	138.8±27.6	159.6±42.8	
	4) Biomass burning	34.5±2.3	16.3±5.7	28.5±3.6	19.1±7.9	17.3±7.9	14.8±5.4	
	5) Rice cultivation		45.4±16.8	86.3±21.0	26.3±5.6	33.0±2.0	28.9±7.6	
	6) Manure management		7.8±0.2		7.9±0.1		8.0±0.3	
	7) Ruminant		64.8±2.2		66.0±0.9		70.0±3.3	
	8) Landfill and Waste		33.6±2.3		39.5±2.0		44.7±3.3	
	Agriculture & Waste*	156.0±12.4	151.6±17.1	179.3±45.4	139.7±6.0	168.8±26.4	151.6±9.0	
	Net CH₄ flux	327.0±45.7	336.5±38.7	324.0±46.6	311.3±39.5	324.8±38.6	325.9±43.3	
	Pre-industrial CH₄ emission	125.4±14.4						
	Human-induced CH₄ flux	201.6±48.1	211.0±41.3	199.6±48.8	185.8±42.1	199.4±41.2	200.5±45.7	
CH ₄ (Tg C/yr)	1) Natural soil		7.9±1.3	6.6±0.5	8.2±1.3	7.5±0.4	8.4±0.9	
	2) Biomass burning		0.7±0.1	0.7±0.1	0.7±0.1	0.6±0.1	0.6±0.2	
	3) Agricultural soil		2.6±0.3		3.3±0.2		4.0±0.3	
	4) Manure management		0.2±0.0		0.2±0.0		0.3±0.0	
	5) Indirect emission		0.5±0.1		0.9±0.1		0.7±0.1	
	6) Human Sewage		0.2±0.6		0.2±0.0		0.3±0.0	
		Agriculture & Waste *	4.7±4.2	4.1±0.6	4.6±0.2	4.4±0.6	5.5±0.7	
		Net N₂O flux		14.0±4.3	11.3±0.8	14.3±0.9	12.6±0.7	15.2±1.0
		Pre-industrial N₂O emission	7.4±1.3					
		Human-induced N₂O flux		6.6±4.5	3.9±1.5	6.9±1.6	5.2±1.5	7.8±1.6
N ₂ O (Tg N/yr)	1) Natural soil		7.9±1.3	6.6±0.5	8.2±1.3	7.5±0.4	8.4±0.9	
	2) Biomass burning		0.7±0.1	0.7±0.1	0.7±0.1	0.6±0.1	0.6±0.2	
	3) Agricultural soil		2.6±0.3		3.3±0.2		4.0±0.3	
	4) Manure management		0.2±0.0		0.2±0.0		0.3±0.0	
	5) Indirect emission		0.5±0.1		0.9±0.1		0.7±0.1	
	6) Human Sewage		0.2±0.6		0.2±0.0		0.3±0.0	
		Agriculture & Waste *	4.7±4.2	4.1±0.6	4.6±0.2	4.4±0.6	5.5±0.7	
		Net N₂O flux		14.0±4.3	11.3±0.8	14.3±0.9	12.6±0.7	15.2±1.0
		Pre-industrial N₂O emission	7.4±1.3					
		Human-induced N₂O flux		6.6±4.5	3.9±1.5	6.9±1.6	5.2±1.5	7.8±1.6

Estimates are derived from top-down and bottom-up approaches. The complete set of data used for these calculations can be found in Supplementary Table 2.

*Additional data sources are included in the calculation of GHG fluxes for this sub-total sector. Therefore, the sub-total GHG fluxes are not necessarily equal to the sum of individual sector values shown in this table.